

Decadal seesaw of the Central and Subtropical Mode Water formation associated with the Kuroshio Extension variability

Eitarou Oka · Bo Qiu · Shinya Kouketsu ·
Kazuyuki Uehara · Toshio Suga

Received: 30 September 2011 / Revised: 14 December 2011 / Accepted: 20 December 2011 / Published online: 20 January 2012
© The Oceanographic Society of Japan and Springer 2012

Abstract Available Argo profiling float data from 2002 to 2011 were analyzed to examine the effect of the Kuroshio Extension (KE) current system variability on the formation of the Central Mode Water. Just north of the upstream portion of the KE at 140–152°E, formation of a lighter variety of the Central Mode Water in winter was active during the unstable period of the upstream KE in 2006–2009 and was reduced when the upstream KE was in the stable period of 2002–2005 and 2010–2011. This decadal formation variability is out of phase with that of the Subtropical Mode Water just south of the KE.

Keywords Decadal variability · North Pacific · Mode waters · Kuroshio Extension · Mesoscale eddies

E. Oka (✉)
Atmosphere and Ocean Research Institute,
The University of Tokyo, Kashiwa 277-8564, Japan
e-mail: eoka@ori.u-tokyo.ac.jp

B. Qiu
Department of Oceanography, University of Hawaii at Manoa,
Honolulu, HI 96822, USA

S. Kouketsu · T. Suga
Research Institute for Global Change,
Japan Agency for Marine-Earth Science and Technology,
Yokosuka 237-0061, Japan

K. Uehara
Department of Marine Science, School of Marine Science
and Technology, Tokai University, Shizuoka 424-8610, Japan

T. Suga
Department of Geophysics, Graduate School of Science,
Tohoku University, Sendai 980-8578, Japan

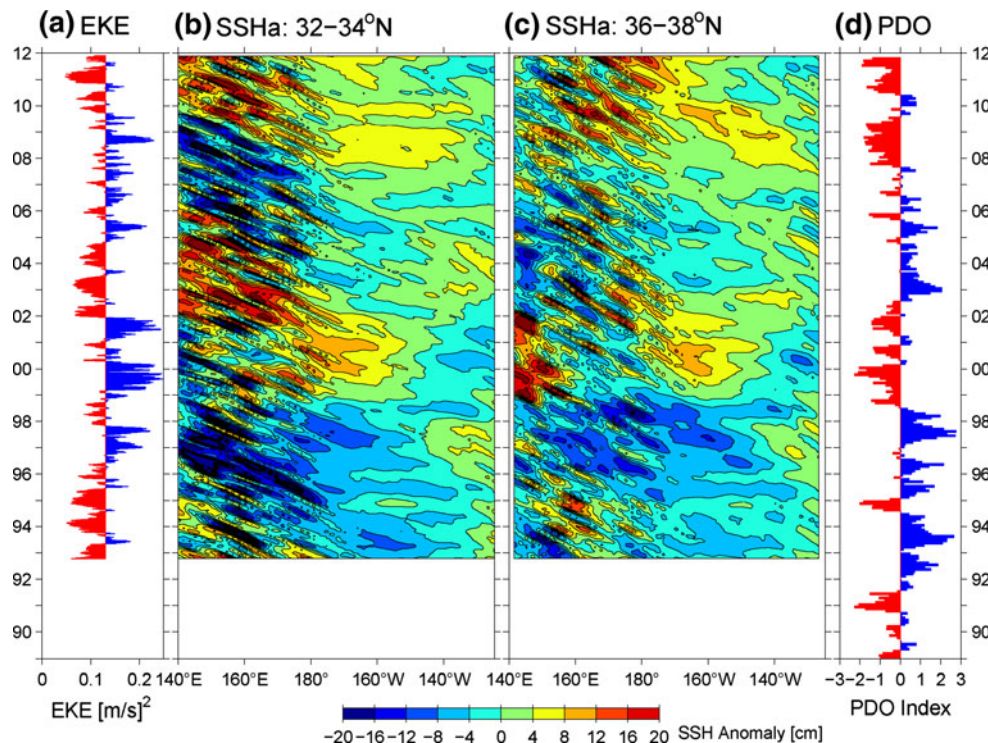
1 Introduction

Accumulation of satellite altimeter sea surface height data over the past 19 years has revealed decadal variability of the Kuroshio Extension (KE) jet and its associated mesoscale eddy field (Qiu and Chen 2005, 2011; Qiu et al. 2007). This decadal variability is remotely forced by large-scale wind stress curl forcing in the central North Pacific centered at 40°N, 160°W (Qiu 2003; Taguchi et al. 2007), whose strength fluctuates in association with the Pacific decadal oscillations (PDOs; Mantua et al. 1997). Specifically, when the PDO index is positive (negative), negative (positive) sea surface height and permanent thermocline depth anomalies are generated and propagate westward at the speed of first-mode baroclinic Rossby waves. When the wind-induced negative (positive) anomalies reach the region east of Japan, the KE jet weakens (strengthens), accompanied by a weak (strong) southern recirculation gyre and high (low) regional eddy activity (Fig. 1a, b, d).¹ During its weakened (strengthened) period, the KE jet is unstable (stable) in its upstream portion at 140–152°E and stable (unstable) in its downstream portion at 152–165°E.

The decadal KE variability has recently been recognized to exert a significant impact on various processes of neighboring water masses, thanks to the development of the Argo profiling float array (Roemmich et al. 2009; Freeland et al. 2010). In contrast with our traditional view that the mode water thickness is determined by the surface heat flux forcing, thinner (thicker) Subtropical Mode Water (STMW; Masuzawa 1969) is formed as deep winter mixed layer in the southern recirculation gyre when the upstream KE is in the unstable (stable) state (Qiu and Chen 2006).

¹ The sea surface height anomalies along 32–34°N best explain the relation between the PDOs and the KE system variability.

Fig. 1 **a** Time series of eddy kinetic energy (EKE) in the upstream KE region of 32–38°N, 141–153°E. Here, EKE is calculated using the weekly sea surface height anomalies from the satellite altimeter data compiled by the Collecte Localisation Satellites (CLS) Space Oceanographic Division of Toulouse, France (Ducet et al. 2000). **b, c** Sea surface height anomalies (SSHa) along the zonal bands of **b** 32–34°N and **c** 36–38°N. **d** PDO index from the Joint Institute for the Study of the Atmosphere and Ocean Web site (available online at <http://jisao.washington.edu/pdo/PDO.latest>)



This is because during an unstable period, both the active southward transport of high potential vorticity water from the Mixed Water region across the KE due to stronger eddy activity (Qiu and Chen 2006; Qiu et al. 2007) and the higher background stratification associated with the shallower permanent pycnocline in the recirculation gyre (Sugimoto and Hanawa 2010) are unfavorable for the development of deep winter mixed layers. The decadal KE variability also affects the STMW circulation (Oka et al. 2011a) and possibly its dissipation (Oka and Qiu 2012). In addition to STMW, the decadal KE variability also influences the modulation of the North Pacific Intermediate Water (NPIW; Reid 1965). NPIW south of the downstream KE was fresher during 2002–2005 (when the downstream KE was unstable and the upstream KE was stable) than 2006–2009 (the opposite phase), because the stronger eddy activity along the downstream KE during the former period led to a larger transport of fresh water from the Mixed Water region in the NPIW density range, while the stronger upstream KE acted as a barrier for the meridional water exchange during both periods (Qiu and Chen 2011).

Motivated by these recent observational studies, it is natural to ask whether the decadal KE variability also affects water mass formation/transformation processes north of the KE. The structure of deep winter mixed layer in the mode water formation regions north of the KE has been recently described using Argo float data from 2003–2008 (Oka et al. 2011b; Fig. 2a). Specifically, two zonally elongated regions of deep winter mixed layer

extend along 33–39°N and 39–43°N from the east coast of Japan to 160°W; the southern region corresponds to the formation region of the lighter variety of Central Mode Water (L-CMW; Tsujino and Yasuda 2004; Oka and Suga 2005), and the northern region to those of the denser variety of Central Mode Water (D-CMW) and the Transition Region Mode Water (TRMW; Saito et al. 2007). On the other hand, an ongoing analysis of dense shipboard observation data north of the KE in spring 2003 (Oka et al., manuscript in preparation) found no L-CMW in the western part of its formation region west of 160°E. This suggests a large temporal variability in the L-CMW formation with the possibility of its relation to the decadal KE variability.

The aforementioned study by Oka et al. (2011b) analyzed the float data from both periods of the KE stability to describe the deep winter mixed layer structure in the mode water formation regions. In this paper, we reexamine the mixed layer structures using the data from 2002–2011, focusing on the differences between the stable versus unstable periods of the KE.

2 Results

Temperature and salinity data of 2002–2011 from the Argo profiling floats, downloaded from the ftp site of the Argo Global Data Assembly Center and edited as outlined in Oka et al. (2007), are used to plot the mixed layer depths

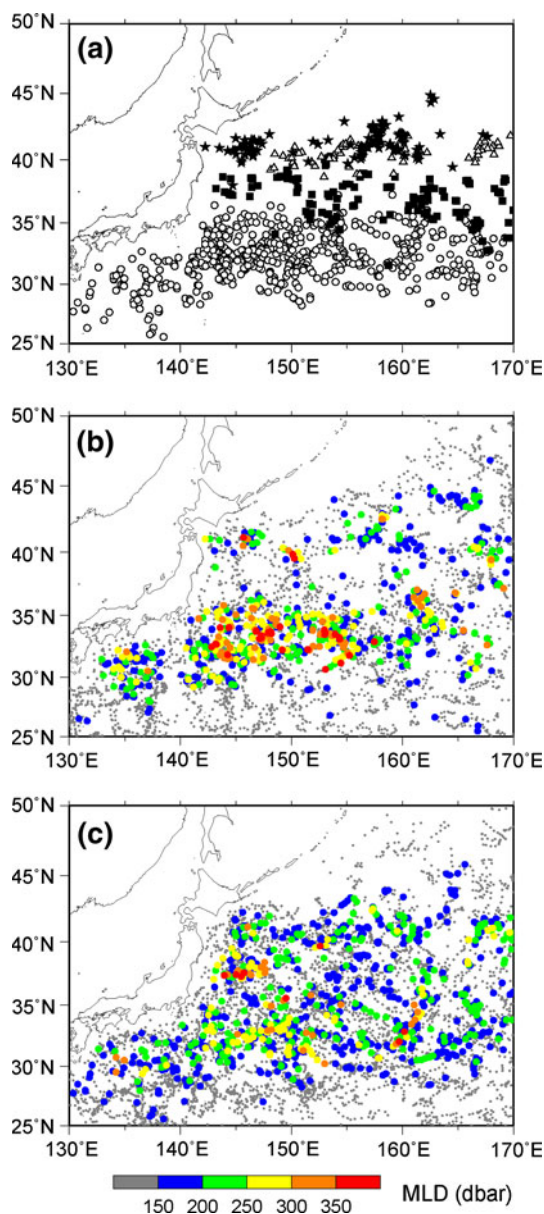


Fig. 2 **a** Distributions of mixed layers deeper than 150 dbar with the properties of STMW (*white circles*), L-CMW (*black squares*), D-CMW (*white triangles*), and TRMW (*black stars*), based on the float data in February–April of 2003–2008 (adapted from Oka et al. 2011b). **b, c** Distributions of MLD in February–April of **b** 2002–2005, 2010–2011 and **c** 2006–2009 from the float data. Note that *gray dots* for MLD <150 dbar are smaller than the other *dots*

(MLDs) in late winter months of February–April for the stable (2002–2005, 2010–2011) and unstable (2006–2009) periods of the upstream KE (Fig. 2b, c). Here, MLD is defined as the shallower value of the depth at which the potential density increases by 0.03 kg m^{-3} from 10-dbar depth and that at which the potential temperature changes by 0.2°C from 10-dbar depth, following the definition of de Boyer Montégut et al. (2004) and Oka et al. (2007). During the unstable period, deep mixed layers (>150 dbar) were

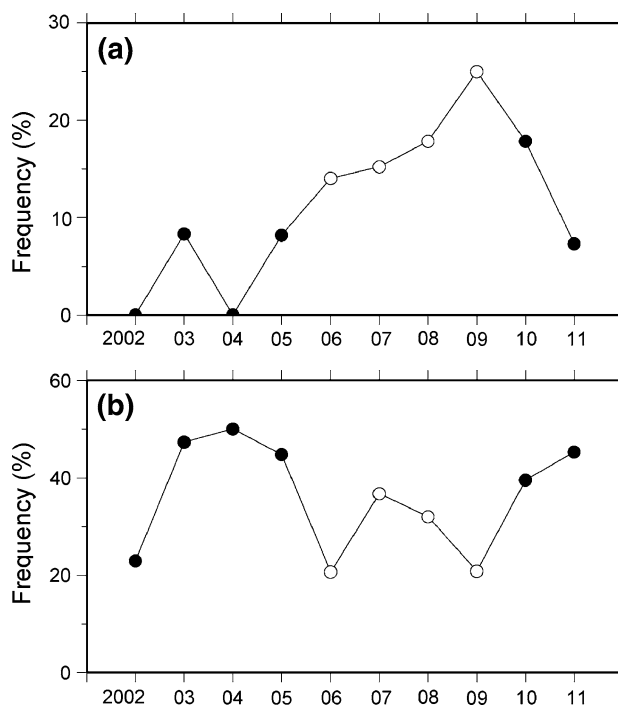


Fig. 3 Time series of frequency of MLD greater than 150 dbar at **a** $36\text{--}40^\circ\text{N}$, $140\text{--}155^\circ\text{E}$ and **b** $31\text{--}35^\circ\text{N}$, $140\text{--}155^\circ\text{E}$ in February and March from the float data. *Black (white) circles* correspond to the period when the upstream KE was stable (unstable)

formed all over the region east of Japan between 28° and 43°N (Fig. 2c), as demonstrated by Oka et al. (2011b) for the period of 2003–2008 (Fig. 2a). In contrast, during the stable period, there was a gap of deep mixed layers at $36\text{--}40^\circ\text{N}$, west of 158°E (Fig. 2b). This area, located just north of the KE ($\sim 35^\circ\text{N}$), corresponds to the western part of the L-CMW formation region (Oka et al. 2011b; Fig. 2a), as confirmed by plotting temperature, salinity, and density distributions for the deep mixed layers (not shown). The time series of frequency of deep mixed layers in this area exhibits a clear tendency of relatively high values during the unstable period and low values during the stable period (Fig. 3a). The averaged frequency of deep mixed layers during the unstable period (18.0%) is more than twice as high as that during the stable period (7.0%). Such a tendency in the western part of the L-CMW formation region is consistent with the nonexistence of L-CMW in spring 2003 during the stable period (Oka et al., manuscript in preparation), and is opposite to that in the STMW formation region between 140° and 155°E where deep winter mixed layers were more frequently observed during the stable period than the unstable period (Figs. 2, 3b).

The winter MLD maps composited for the two periods highlight the impact of the decadal KE variability on the mode water formation. During the stable period, MLD was large east of Japan at $31\text{--}35^\circ\text{N}$ and $40\text{--}42^\circ\text{N}$,

corresponding to the formation regions of STMW and D-CMW/TRMW, respectively, while it had a minimum at 36–39°N, reflecting the inactive L-CMW formation (Fig. 4a). During the unstable period, on the other hand, three comparable maxima of MLD existed in the three mode water formation regions at 30–33°N and 37–39°N east of Japan and at 40–43°N, 154–162°E, and the meridional contrast of MLD was much smaller than during the stable period (Fig. 4b). The composite MLD difference between the two periods delineates a striking dipole pattern sandwiching the KE between 140° and 155°E, indicating

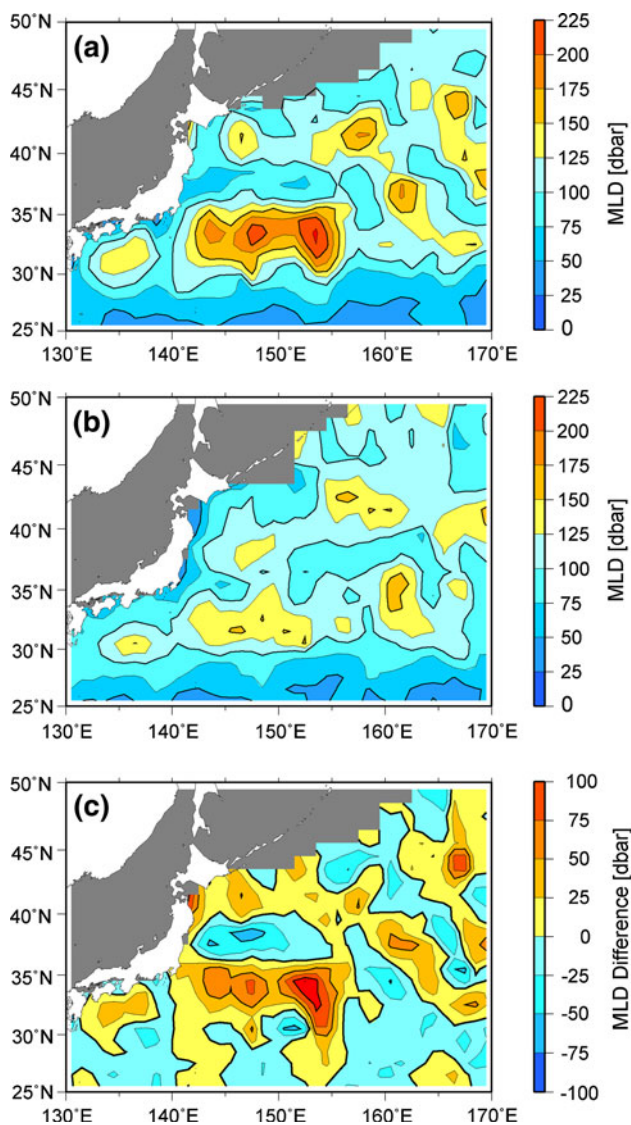


Fig. 4 Distributions of MLD in February and March of **a** 2002–2005, 2010–2011 and **b** 2006–2009, averaged for each $1^\circ \times 1^\circ$ grid box using the float data from a $3^\circ \times 3^\circ$ grid box centered by the $1^\circ \times 1^\circ$ grid box and weight function of d^{-2} (d is the distance in degree from the center of the $1^\circ \times 1^\circ$ grid box) for observation points where $d > 1^\circ$. **c** Difference of the averaged MLD between **a** and **b** (former minus latter)

enhanced formation of STMW during the stable period and of L-CMW during the unstable period (Fig. 4c).

3 Discussion

The above analyses demonstrated that the L-CMW production in the western part of its formation region is high (low) during the unstable (stable) period of the upstream KE and is out of phase with the STMW production on the southern side of the KE. Since this variability occurs in almost the same longitude range as the upstream KE variability (140–152°E), its mechanism can be reasonably explained as follows. During the unstable period, the regional eddy activity is high along the upstream KE, where nonlinear anticyclonic eddies actively detach from the KE to its north. These eddies bring low potential vorticity water of the southern recirculation gyre into the L-CMW formation region, reduce the background stratification in the L-CMW formation region by increasing the average permanent pycnocline depth, and generate a pre-condition favorable for deep winter mixed layer development. In addition, these eddies themselves have been recently considered as important formation sites of L-CMW. A composite analysis of Argo float data and satellite sea surface height data demonstrated that roughly half of deep winter mixed layers in the L-CMW formation region are formed inside the anticyclonic eddies (Kouketsu et al. 2012). This result is supported by past shipboard observations (Tomosada 1986; Yasuda et al. 1992) revealing that while the anticyclonic eddies detached from the KE survive through winter in the Mixed Water region, the southern-origin STMW trapped within them is modified to L-CMW because of the convective winter cooling and interaction with the ambient water. Moreover, during an unstable period, the KE tends to take a southerly position and the Kuroshio bifurcation front tends to develop (Qiu and Chen 2011), which also provides a favorable environment for the L-CMW formation. Thus, the KE variability has an opposite effect on the deep winter mixed layer development between the L-CMW and STMW formation regions. In the latter region, the enhanced eddy activity during the unstable period inhibits the mixed layer development because the eddies bring high potential vorticity water from the Mixed Water region (Qiu and Chen 2006; Qiu et al. 2007).

Given the large spatial scale of atmospheric forcing, the wind stress curl forcing in the central North Pacific generates sea surface height (and permanent pycnocline depth) anomalies of the same sign near 160°W in both latitude ranges of 32–34°N and 36–38°N corresponding to the STMW and L-CMW formation regions, respectively (Fig. 1b–d). The anomalies generated at 36–38°N

propagate westward at a lower speed and tend to reach 150°E roughly a year later than those at 32–34°N because of the smaller Coriolis parameter and weaker stratification (e.g., Qiu 2003). If they extend all the way to the east coast of Japan, the wind-induced anomalies are expected to raise (lower) the permanent pycnocline and enhance (reduce) the background stratification in the L-CMW formation region during an unstable (stable) period, therefore weakening the decadal L-CMW formation variability. However, the propagating anomalies along 36–38°N change their sign near the east coast of Japan and turn positive (negative) during the unstable (stable) period (Fig. 1c). Such a reversal of anomalies is not observed along 32–34°N (Fig. 1b), and is likely due to the more (less) active detachment of nonlinear anticyclonic eddies from the KE during the unstable (stable) period. Thus, in the western part of the L-CMW formation region, the sea surface height and permanent pycnocline depth anomalies appear to be more determined by the nonlinear eddy signals relating to the decadal varying KE stability than by the wind-induced sea surface height anomalies propagating from the east.² It is this dominance by eddy signals that is responsible for the observed decadal seesaw between the L-CMW and STMW changes.

It might be worth noting that during the stable period, the winter mixed layer is deeper in the region between 40° and 42°N, west of 160°E, which corresponds to the formation region of D-CMW and TRMW (mostly the latter in this longitude range; Figs. 2a, 4c). This seems to be consistent with the following findings in recent years: thick TRMW is locally formed just south of a quasistationary jet associated with the subarctic front (Isoguchi et al. 2006; Saito et al. 2007; Tomita et al. 2011); the jet is stronger (weaker) when the upstream KE takes a northerly (southerly) position (T. Wagawa, personal communication); and the upstream KE tends to take a northerly (southerly) position during the stable (unstable) period (Qiu and Chen 2011). There might be a relation that during the stable period, the stronger quasistationary jet transports more warm water from the south, enhances the deep winter convection to its south, and leads to the formation of thicker TRMW.

The decadal L-CMW formation variability identified in this study has a wide range of implications from the physical and biogeochemical perspectives. Changes in the L-CMW formation alter the upper thermal structure in the Mixed Water region, which can modulate the sea surface temperature and possibly feedback onto the atmosphere. Through

changes in winter MLD, the L-CMW formation variability can affect subsurface dissolved oxygen distribution and air-to-sea CO₂ flux that is high in the mode water formation regions in winter (Takahashi et al. 2009). Moreover, a deeper (shallower) winter mixed layer in the L-CMW formation region might lead to a larger (smaller) nutrient supply from deeper layers during the unstable (stable) period, although this vertical transport effect might be cancelled out by the horizontal transport of more (less) oligotrophic water from the southern recirculation gyre.

In addition to these local effects, the influence of the decadal L-CMW formation variability in the western part of its formation region on the L-CMW formation and subduction in the eastern part of the formation region (Oka et al. 2011b), and further on the upper thermal structure in the subtropical gyre and decadal climate variability in the Pacific region, needs to be examined in future studies. If L-CMWs are largely formed in nonlinear anticyclonic eddies, they are not likely to be advected eastward by the mean flow, as speculated by Oka et al. (2011b), but move westward as isolated eddies (Itoh and Yasuda 2010). The standard density of Argo floats (one float per 3° square) is obviously insufficient to study detailed processes of how the eddies contribute to the L-CMW formation and subduction. High-resolution shipboard observations (e.g., Oka et al. 2009, 2011a) and concentrated deployment of the profiling floats in the L-CMW formation region in combination with eddy-resolving ocean general circulation models are strongly desired.

Acknowledgments The authors thank Tsuyoshi Ohira for help in preparing the Argo float data and two anonymous reviewers for helpful comments on the manuscript. The Argo float data used in this study were collected and made freely available by the International Argo Project and the national programs that contribute to it (<http://www.argo.ucsd.edu>, <http://argo.jcommops.org>). This study was motivated by discussions between EO and BQ in summer 2010 when EO visited the University of Hawaii at Manoa for 1 month under the Overseas Internship Program for Outstanding Young Earth and Planetary Researchers provided by the Department of Earth and Planetary Science, the University of Tokyo. EO, KU, and TS are supported by the Japan Society for Promotion of Science (KAKENHI, Grant-in-Aid for Scientific Research (B), no. 21340133) and the Ministry of Education, Culture, Sports, Science and Technology, Japan (MEXT; Grant-in-Aid for Scientific Research on Innovative Areas under grant no. 22106007). BQ is supported by NSF through Grant OCE-0220680 and NASA through contract 1207881.

References

- de Boyer Montégut C, Madec G, Fischer AS, Lazar A, Iudicone D (2004) Mixed layer depth over the global ocean: an examination of profile data and a profile-based climatology. *J Geophys Res* 109:C12003. doi:10.1029/2004JC002378
- Ducet N, Le Traon PY, Reverdin F (2000) Global high-resolution mapping of ocean circulation from TOPEX/Poseidon and ERS-1 and -2. *J Geophys Res* 105:19477–19498

² In the STMW formation region, the sea surface height anomalies propagating from the east and those due to the nonlinear eddy signals have the same sign, which explains why the reversal of anomalies was not observed there.

- Freeland H et al (2010) Argo—a decade of progress. In: Hall J, Harrison DE, Stammer D (eds) *Proceedings of OceanObs'09: sustained ocean observations and information for society*, 21–25 September 2009, vol 2. ESA publication WPP-306, Venice. doi: [10.5270/OceanObs09.cwp.32](https://doi.org/10.5270/OceanObs09.cwp.32)
- Isoguchi O, Kawamura H, Oka E (2006) Quasi-stationary jets transporting surface warm waters across the transition zone between the subtropical and the subarctic gyres in the North Pacific. *J Geophys Res* 111:C10003. doi: [10.1029/2005JC003402](https://doi.org/10.1029/2005JC003402)
- Itoh S, Yasuda I (2010) Characteristics of mesoscale eddies in the Kuroshio–Oyashio Extension region detected from the distribution of the sea surface height anomaly. *J Phys Oceanogr* 40:1018–1034
- Kouketsu S, Tomita H, Oka E, Hosoda S, Kobayashi T, Sato K (2012) The role of meso-scale eddies in mixed layer deepening and mode water formation in the western North Pacific. *J Oceanogr* 68:63–77
- Mantua NJ, Hare SR, Zhang Y, Wallace JM, Francis RC (1997) A Pacific interdecadal climate oscillation with impacts on salmon production. *Bull Am Meteorol Soc* 78:1069–1079
- Masuzawa J (1969) Subtropical Mode Water. *Deep Sea Res* 16:463–472
- Oka E, Qiu B (2012) Progress of North Pacific mode water research in the past decade. *J Oceanogr* 68:5–20
- Oka E, Suga T (2005) Differential formation and circulation of North Pacific Central Mode Water. *J Phys Oceanogr* 35:1997–2011
- Oka E, Talley LD, Suga T (2007) Temporal variability of winter mixed layer in the mid- to high-latitude North Pacific. *J Oceanogr* 63:293–307
- Oka E, Toyama K, Suga T (2009) Subduction of North Pacific central mode water associated with subsurface mesoscale eddy. *Geophys Res Lett* 36:L08607. doi: [10.1029/2009GL037540](https://doi.org/10.1029/2009GL037540)
- Oka E, Suga T, Sukigara C, Toyama K, Shimada K, Yoshida J (2011a) “Eddy-resolving” observation of the North Pacific Subtropical Mode Water. *J Phys Oceanogr* 41:666–681
- Oka E, Kouketsu S, Toyama K, Uehara K, Kobayashi T, Hosoda S, Suga T (2011b) Formation and subduction of Central Mode Water based on profiling float data, 2003–08. *J Phys Oceanogr* 41:113–129
- Qiu B (2003) Kuroshio Extension variability and forcing of the Pacific decadal oscillations: responses and potential feedback. *J Phys Oceanogr* 33:2465–2482
- Qiu B, Chen S (2005) Variability of the Kuroshio Extension jet, recirculation gyre and mesoscale eddies on decadal timescales. *J Phys Oceanogr* 35:2090–2103
- Qiu B, Chen S (2006) Decadal variability in the formation of the North Pacific Subtropical Mode Water: oceanic versus atmospheric control. *J Phys Oceanogr* 36:1365–1380
- Qiu B, Chen S (2011) Effect of decadal Kuroshio Extension jet and eddy variability on the modification of North Pacific Intermediate Water. *J Phys Oceanogr* 41:503–515
- Qiu B, Chen S, Hacker P (2007) Effect of mesoscale eddies on subtropical mode water variability from the Kuroshio Extension System Study (KESS). *J Phys Oceanogr* 37:982–1000
- Reid JL (1965) Intermediate Water of the Pacific Ocean. *Johns Hopkins oceanographic studies*, vol 2. The John Hopkins Press, Baltimore, p 58
- Roemmich D, Johnson GC, Riser S, Davis R, Gilson J, Owens WB, Garzoli SL, Schmid C, Ignaszewski M (2009) Argo: the challenge of continuing 10 years of progress. *Oceanography* 22:46–55
- Saito H, Suga T, Hanawa K, Watanabe T (2007) New type of pycnostad in the western subtropical-subarctic transition region of the North Pacific: Transition Region Mode Water. *J Oceanogr* 63:589–600
- Sugimoto S, Hanawa K (2010) Impact of Aleutian low activity on the STMW formation in the Kuroshio recirculation gyre region. *Geophys Res Lett* 37:L03606. doi: [10.1029/2009GL041795](https://doi.org/10.1029/2009GL041795)
- Taguchi B, Xie SP, Schneider N, Nonaka M, Sasaki H, Sasai Y (2007) Decadal variability of the Kuroshio Extension: observations and an eddy-resolving model hindcast. *J Clim* 20:2357–2377
- Takahashi T et al (2009) Climatological mean and decadal change in surface ocean pCO₂, and net sea-air CO₂ flux over the global ocean. *Deep Sea Res* 56:554–577
- Tomita H, Kouketsu S, Oka E, Kubota M (2011) Locally enhanced wintertime air-sea interaction and deep oceanic mixed layer formation associated with the subarctic front in the North Pacific. *Geophys Res Lett* 38:L24607. doi: [10.1029/2011GL049902](https://doi.org/10.1029/2011GL049902)
- Tomosada A (1986) Generation and decay of Kuroshio warm-core rings. *Deep Sea Res* 33:1475–1486
- Tsujino H, Yasuda T (2004) Formation and circulation of mode waters of the North Pacific in a high-resolution GCM. *J Phys Oceanogr* 34:399–415
- Yasuda I, Okuda K, Hirai M (1992) Evolution of a Kuroshio warm-core ring-variability of the hydrographic structure. *Deep Sea Res* 39:S131–S161